J|A|C|S
ARTICLES
Published on Web 01/04/2007

Polyproline-Rod Approach to Isolating Protein Targets of Bioactive Small Molecules: Isolation of a New Target of Indomethacin

Shin-ichi Sato,[†] Youngjoo Kwon,[†,§] Shinji Kamisuki,[†] Neeta Srivastava,[†] Qian Mao,[†] Yoshinori Kawazoe,[†,‡] and Motonari Uesugi*[†,‡]

Contribution from The Verna and Marrs McLean Department of Biochemistry and Molecular Biology, Baylor College of Medicine, Houston, Texas 77030, and Institute for Chemical Research, Kyoto University, Uji, Kyoto 611-0011, Japan

Received August 1, 2006; E-mail: muesugi@bcm.tmc.edu

Abstract: Identification of protein targets of bioactive small molecules has been a technical hurdle of chemical genetics. Here we report a polyproline-rod approach to isolating protein targets of small molecules from cell lysates. The results indicate that insertion of a long, rigid polyproline helix between a small-molecule bait and a biotin tag boosts the capacity of affinity purification and thereby permits isolation of low-abundance or low-affinity proteins. In the course of the proof-of-concept experiments, we isolated glyoxalase 1 (GLO1) as a new target of indomethacin, a widely used antiinflammatory drug. Molecular biological experiments suggest that inhibition of GLO1 enzyme activity is related to the clinically recognized beneficial side effects of the indomethacin family of nonsteroidal antiinflammatory drugs.

Introduction

One of the technical challenges in forward chemical genetics and phenotype-based drug discovery is the identification of protein targets of bioactive small molecules.[1] The most straightforward approach to identifying protein targets is biochemical isolation with affinity resins, in which a close analogue of a small-molecule ligand is covalently attached to a solid support,[2−5] or its biotinylated version is bound to avidin-agarose beads.[6−13] The avidin−biotin affinity approach is based on the remarkably strong noncovalent interaction between biotin and avidin and has been offering a convenient preparation of affinity columns of bioactive molecules since its introduction in 1976 by Hofmann and co-workers.[14,15]

One problem of the widely used avidin−biotin approach is the low recovery of binding proteins relative to a high-density direct conjugation approach. The crystal structure of avidin bound to biotin indicates that biotin binds within a deep cleft inside the core of avidin, and the distance from the bound biotin molecule to the surface of avidin is as long as 7 Å.[16,17] Commercially available biotinylation reagents are usually composed of relatively short methylene or ethylene glycol linkers (up to 14 Å) and may not project the small-molecule ligand away enough for the isolation of bulky binding proteins. A longer linker with optimized chemical and physical properties would be desirable.

Our approach to designing such a linker stems from the analogy of affinity purification to fishing, in which a rod is often used to cast a fishhook away and to prevent tangles of fishing lines. In our design, a rod-like polyproline helix is inserted between a small-molecule bait and a biotin molecule. The stretch of L-prolines forms a stable left-handed helix, and the length of the 9-proline helix has been measured to be 27 Å by fluorescence resonance energy transfer experiments.[18,19] The rigid polyproline helix may prevent folding of the linker and project

[†] Baylor College of Medicine.
[‡] Kyoto University.
[§] Current address: College of Pharmacy, Ewha Womans University, Seoul 120-750, Korea.

(1) Burdine, L.; Kodadek, T. *Chem. Biol.* **2004**, *11*, 593−597.
(2) Harding, M. W.; Galat, A.; Uehling, D. E.; Schreiber, S. L. *Nature* **1989**, *341*, 758−760.
(3) Taunton, J.; Hassig, C. A.; Schreiber, S. L. *Science* **1996**, *272*, 408−411.
(4) Ding, S.; Wu, T. Y.; Brinker, A.; Peters, E. C.; Hur, W.; Gray, N. S.; Schultz, P. G. *Proc. Natl. Acad. Sci. U.S.A.* **2003**, *100*, 7632−7637.
(5) Khersonsky, S. M.; Jung, D. W.; Kang, T. W.; Walsh, D. P.; Moon, H. S.; Jo, H.; Jacobson, E. M.; Shetty, V.; Neubert, T. A.; Chang, Y. T. *J. Am. Chem. Soc.* **2003**, *125*, 11804−11805.
(6) Lefkowitz, R. J.; Haber, E.; O'Hara, D. *Proc. Natl. Acad. Sci. U.S.A.* **1972**, *69*, 2828−2832.
(7) Sin, N.; Meng, L.; Wang, M. Q.; Wen, J. J.; Bornmann, W. G.; Crews, C. M. *Proc. Natl. Acad. Sci. U.S.A.* **1997**, *94*, 6099−6103.
(8) Meng, L.; Mohan, R.; Kwok, B. H.; Elofsson, M.; Sin, N.; Crews, C. M. *Proc. Natl. Acad. Sci. U.S.A.* **1999**, *96*, 10403−10408.
(9) Nguyen, C.; Teo, J. L.; Matsuda, A.; Eguchi, M.; Chi, E. Y.; Henderson, W. R., Jr.; Kahn, M. *Proc. Natl. Acad. Sci. U.S.A.* **2003**, *100*, 1169−1173.
(10) Shim, J. S.; Lee, J.; Park, H. J.; Park, S. J.; Kwon, H. J. *Chem. Biol.* **2004**, *11*, 1455−1463.
(11) Shimogawa, H.; Kwon, Y.; Mao, Q.; Kawazoe, Y.; Choi, Y.; Asada, S.; Kigoshi, H.; Uesugi, M. *J. Am. Chem. Soc.* **2004**, *126*, 3461−3471.
(12) Sche, P. P.; McKenzie, K. M.; White, J. D.; Austin, D. J. *Chem. Biol.* **1999**, *6*, 707−716.
(13) Choi, Y.; Shimogawa, H.; Murakami, K.; Ramdas, L.; Zhang, W.; Qin, J.; Uesugi, M. *Chem. Biol.* **2006**, *13*, 241−249.
(14) Hofmann, K.; Finn, F. M.; Kiso, Y. *J. Am. Chem. Soc.* **1978**, *100*, 3585−3590.
(15) Hofmann, K.; Kiso, Y. *Proc. Natl. Acad. Sci. U.S.A.* **1976**, *73*, 3516−3518.
(16) Pugliese, L.; Coda, A.; Malcovati, M.; Bolognesi, M. *J. Mol. Biol.* **1993**, *231*, 698−710.
(17) Livnah, O.; Bayer, E. A.; Wilchek, M.; Sussman, J. L. *Proc. Natl. Acad. Sci. U.S.A.* **1993**, *90*, 5076−5080.
(18) Arora, P. S.; Ansari, A. Z.; Best, T. P.; Ptashne, M.; Dervan, P. B. *J. Am. Chem. Soc.* **2002**, *124*, 13067−13071.
(19) Stryer, L.; Haugland, R. P. *Proc. Natl. Acad. Sci. U.S.A.* **1967**, *58*, 719−726.

a small-molecule bait away from the biotin−avidin complex to permit its interaction with protein targets.

Here we demonstrate that the rigid polyproline linker facilitates the biochemical isolation of protein targets. During the course of the proof-of-concept experiments, we were able to isolate glyoxalase 1 (GLO1) as a new target of indomethacin, a clinically used nonsteroidal antiinflammatory drug that is known to inhibit cyclooxygenases. Although the generality of the approach needs to be addressed by many other molecules, the results may suggest the utility of rod-like linkers in increasing the success rates of biochemically isolating protein targets of small molecules.

Results

Proof of Concept with Glutathione. The small molecule that we initially used for proof of concept was glutathione, a naturally occurring peptide that binds specifically to glutathione-*S*-transferase (GST). Biotinylated glutathione with varied lengths of polyproline linkers (zero, six, and nine L-prolines) were synthesized (Figure 1A) and incubated with *E. coli* cell lysates containing GST. While commercially available glutathione-sepharose, in which a high density of glutathione molecules are attached directly to the solid resin, works well in general due to its high effective concentration, the biotinylated glutathione with a methylene linker (**1**) bound to the avidin agarose resin showed the limited ability to recover GST from the lysates (Figure 1B), representing the low-recovery problem of the avidin−biotin affinity approach. In contrast, when a polyproline linker (**2** or **3**) was inserted between glutathione and biotin, the recovery rates of GST went up, and a longer 9-proline linker (27 Å) showed a higher recovery than the one with six prolines (18 Å) (Figure 1B).

To compare the polyproline linker with poly(ethylene glycol) (PEG) linkers, water-soluble linkers widely used for affinity purification, a series of PEG-based linkers with varied lengths (**4**−**7**; 11−32 Å) were inserted between glutathione and biotin. The longer PEG linkers exhibited the higher recovery of GST from the lysates. However, even the longest PEG linker (**7**, 32 Å) purified ∼1/4 times less GST than the 27-Å polyproline linker (**3**) (Figure 1B). These results encouraged us to pursue the idea of employing a proline-helix linker, rather than flexible linkers, for isolating protein targets.

Proof of Concept with Indomethacin. We next used indomethacin (**8**) as a model of more drug-like organic compounds. Indomethacin is a clinically used antiinflammatory drug that targets cyclooxygenases (COXs) and thereby inhibits the biosynthesis of prostaglandins. As is often with small-molecule drugs, biotin−indomethacin conjugates had limited water solubility, rendering them hard to purify by reversed-phase HPLC. To improve the water-solubility, two lysine residues were introduced between a biotin molecule and a polyproline linker (Figure 2A). The soluble version of the nine-proline-rod−biotin−indomethacin conjugate (**11**) was then examined for its ability to isolate endogenous COX-1 from mammalian cell lysates. Whole cell extracts of mouse STO cells were incubated with conjugate **11**, and bound proteins were analyzed by western blots. As shown in Figure 2B, conjugate **11** had greater ability to isolate COX-1 than control conjugates **9** and **10**. Excess amounts of free indomethacin abolished the interaction between **11** and COX-1 (Figure S1), suggesting that

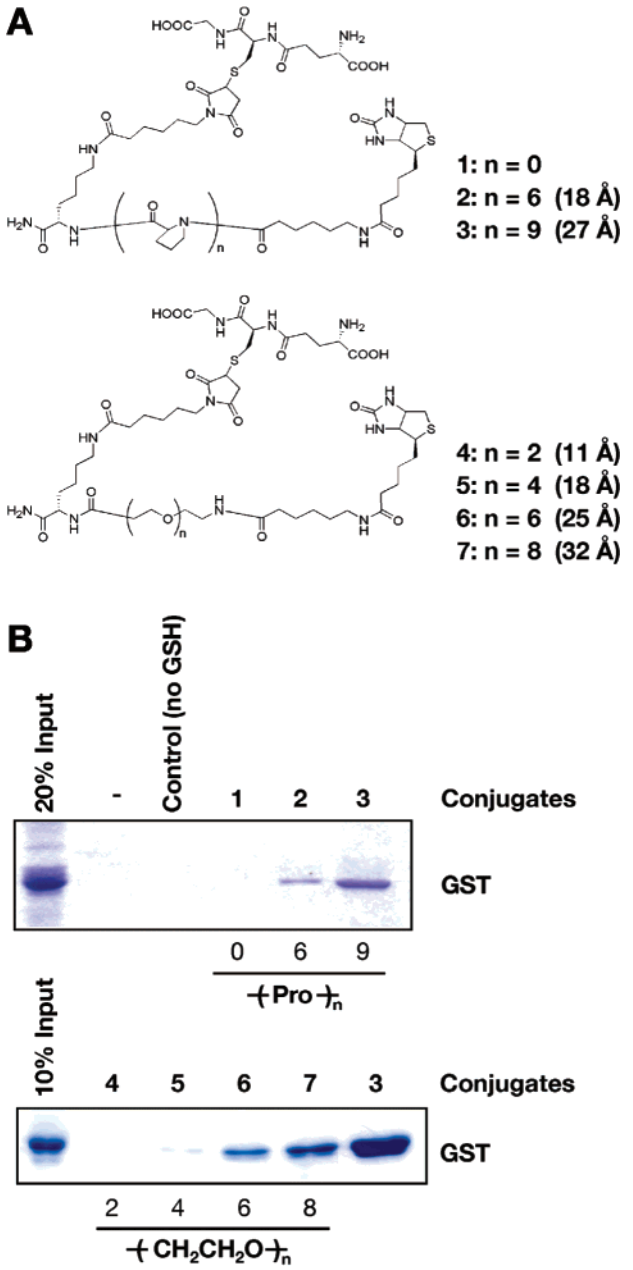

Figure 1. Design of biotinylated glutathione with a polyproline linker. (A) Chemical structures of biotinylated glutathione conjugates **1**−**7**. (B) Affinity purification of GST from bacterial lysates. Increasing amounts of GST were purified by the biotinylated glutathione with a longer proline linker (**2** and **3**) bound to the avidin agarose resin, whereas the one without a polyproline linker (**1**) exhibited only limited ability to purify GST (upper panel). The 27 Å polyproline linker was also compared with polyethylene glycol (PEG) linkers (**4**−**7**) (lower panel). The 27 Å polyproline linker exhibited ∼4 times better recovery of GST than the 32 Å PEG linker.

the interaction is selective. Silver staining of the gel showed a faint but selective protein band whose electrophoretic mobility matched that of COX-1 in the western blots (Figure 2B). To confirm the identity of the band, we scaled up the purification 100 times and excised a Coomassie Blue-stained band from a gel. Microsequencing analysis revealed three peptide sequences that matched the amino-acid sequence of mouse COX-1 (ALGHGVDLGHIYGDNLER, NFDYHVLHVAVDVIK, and QLPDVQLLAQQLLLR). To our knowledge, this result represents the first successful isolation and microsequencing of an

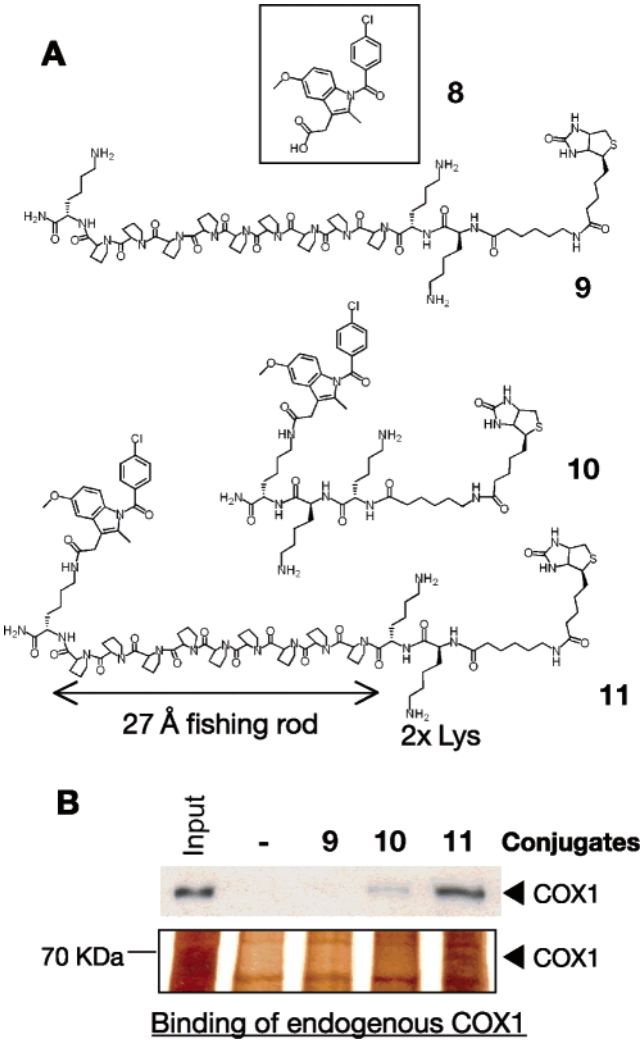

Figure 2. Isolation of COX-1 by a biotinylated proline-rod indomethacin. (A) Structures of indomethacin derivatives and a control compound. (B) Purification of endogenous COX-1 from STO cell lysates. The upper panel shows western blot with a COX-1 antibody. The lower panel shows a silver-stained gel. 20% of input is shown.

endogenous COX protein from mammalian cell lysates by affinity chromatography of a nonsteroidal antiinflammatory drug.

Improvement: Capture and Release. The COX-1 band in Figure 2B is specific but hard to detect due to the overlap with nonspecific bands. Microsequencing of 10 representative nonspecific bands revealed that many of them are associated with the polyproline linker, including proline hydroxylase, 14-3-3, and a number of heat-shock proteins. These nonspecific bands can be removed by taking a capture and release approach, in which a specific protease cleavage site is inserted between a small molecule bait and a proline linker so that the bait and its binding protein can be released by protease cleavage (Figure 3A).

The protease-based capture and release technique is not new in affinity purification in general, but in many cases factor Xa is used as a releasing protease. In our attempt, a 6His-tagged recombinant protein of bacterial HRV-C3 protease was chosen due to its neutral recognition sequence and high activity and

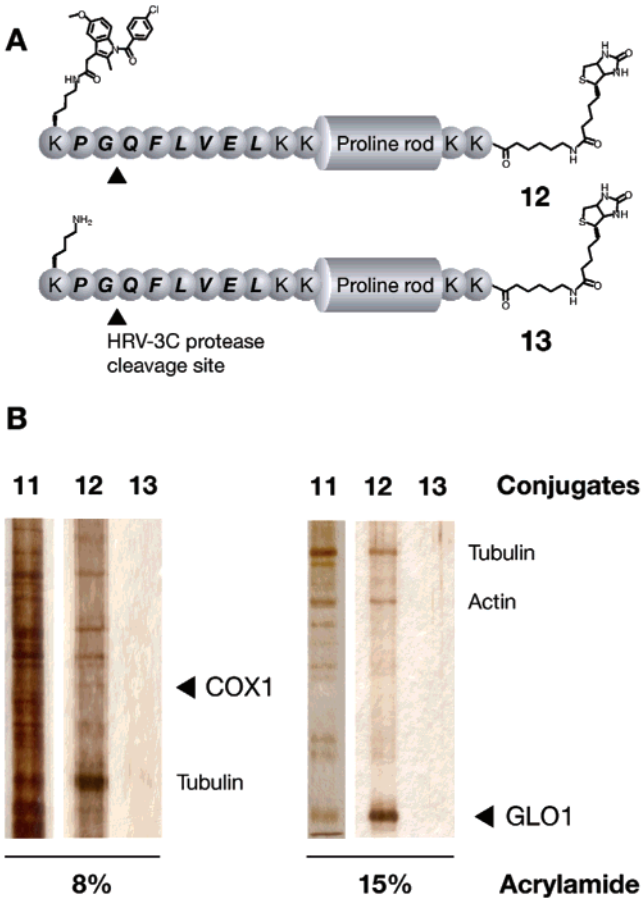

Figure 3. Capture and release of COX-1 and GLO1. (A) Model structures of capture-and-release affinity conjugates. A recognition sequence of HRV-C3 protease is shown in bold italic letters. (B) Isolation of COX-1 and GLO1. The number of nonspecific bands was reduced by proteolytic elution. The loading amounts and staining for **11** and **12** were normalized with the darkest bands on the gels.

selectivity even at 4 °C.[20] The presence of a 6His tag also permits convenient removal of the protease from the sample after cleavage.

Such a capture-and-release version of the indomethacin conjugate **12** was synthesized and tested for the ability to purify COX-1 from STO cell lysates. When a protease-treated sample was analyzed on a silver-stained SDS gel, the number of nonspecific bands was reduced, and, as a result, the COX-1 band became more visible on the gel than it was in a sample eluted simply by SDS (Figure 3B). The combination of the capture-and-release and proline-rod approaches may permit the isolation and detection of the low-abundance proteins that bind to drug-like small molecules.

Identification of Glyoxalase 1 as a Target of Indomethacin. While conducting the capture-and-release experiments with indomethacin, we noticed another specific band in the lower molecular weight region of the gels (Figure 3B). Microsequencing analysis of the band revealed 14 peptide sequences that all matched the amino acid sequence of mouse glyoxalase 1 (GLO1).

GLO1 and structurally unrelated GLO2 forms a metabolic enzyme system that catalyzes the conversion of methyl glyoxal, a cytotoxic metabolite produced primarily as a byproduct of

(20) Cordingley, M. G.; Callahan, P. L.; Sardana, V. V.; Garsky, V. M.; Colonno, R. J. *J. Biol. Chem.* **1990**, *265*, 9062−9065.

Scheme 1. Reactions Catalyzed by the Glyoxalase System

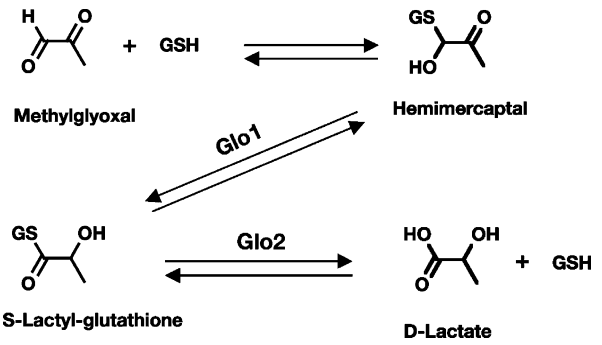

glycolysis, to D-lactate.[21,22] The direct substrate of GLO1 is the hemithioacetal form of methylglyoxal produced by the nonenzymatic conjugation with glutathione, and its product is *S*-D-lactoylglutathione, which is then hydrolyzed by GLO2 to D-lactate (Scheme 1). Notwithstanding the numerous previous studies, GLO1 has never been reported or suggested to be a binding target of indomethacin or any other antiinflammatory drugs.

To examine the effect of indomethacin on the enzymatic activity of GLO1, the catalytic activity of recombinant GLO1 was measured in the presence of varied concentrations of indomethacin. Dixon plot and Lineweaver−Burk plot analyses showed that indomethacin competitively inhibits GLO1 with a K_i value of 18.1 μM (**Figure S2**). This high range of *K*i may still be comparable to the K_i value reported for COX-2 (5 μM), a known pharmacological target of indomethacin, and could be physiological considering a high dose administration of indomethacin in the clinic.[23] When 12 other antiinflammatory drugs that target COX-2 (Figure 4) were evaluated, acemetacin, a close analogue of indomethacin, exhibited comparable inhibitory activity (K_i = 12.1 μM), and other members of indomethacin class of drugs (sulindac, tolmetin, zomepirac) showed weak but detectable activity. In contrast, antiinflammatory drugs of other chemical classes including aspirin, ibuprofen, and Vioxx had little or no detectable effects on GLO1 (Table 1).

A similar trend was observed when K_d was measured by isothermal titration microcalorimetry (ITC). The K_d of indomethacin for GLO1 was estimated to be 4.0 μM with stoichiometry of 1.06 ± 0.08, and zomepirac, which had a five times weaker K_i, exhibited a paralleled K_d (18 μM) (Figure S3). NMR titration experiments indicated that the addition of GLO1 diminished selective proton signals of indomethacin, especially those arising from the methylene (3.53 ppm), 2-methyl (2.18 ppm), and methoxy (3.82 ppm) protons (Figure 5). The signal losses are consistent with the low-μM K_d of the interaction where the exchange rate between the free and bound states is often intermediate at the NMR time scale and the perturbations of the methylene and 2-methyl groups are also in agreement with their importance in the structure−activity relationship for GLO1. [In slow exchange ($<\sim$100 s^{-1}), separate resonances are seen for each of the two states. By contrast, in fast exchange ($>\sim$1000 s^{-1}), a single averaged resonance is observed. In the intermediate exchange region, resonances broaden, often becoming unobservable. Detailed descriptions of these exchange effects in NMR spectra can be found in a number of text books (e.g., Lian, L., Roberts, G. C. K.. In *NMR of Macromolecules. A practical approach*; Roberts, G. C. K., Ed.; Academic Press: London, 1993; pp.153−182).] These biochemical data collectively indicate that, although the potencies vary, the indomethacin family of antiinflammatory drugs interact directly with GL01 and block its enzymatic activity.

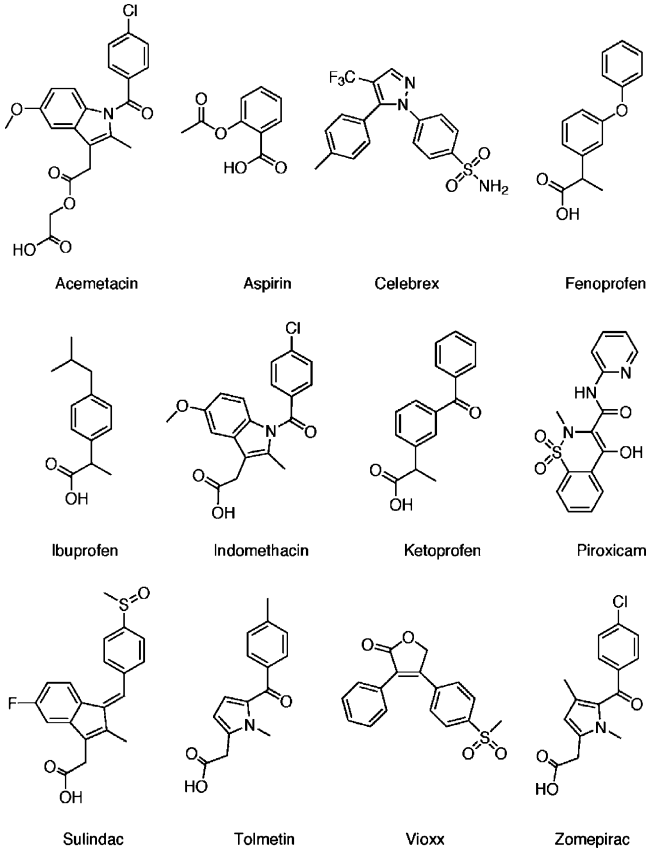

Figure 4. Chemical structures of the nonsteroidal antiinflammatory drugs used in the study.

Table 1. Inhibition of GLO1 with Varied NSAIDS

NSAIDs	K_i[a] (μM)
acemetacin	12.9 ± 0.9
aspirin	>1000
celebrex	>100
fenoprofen	400 (30
ibuprofen	>1000
indomethacin	18.1 ± 0.1
ketoprofen	414 ± 5
piroxicam	808 ± 12
sulindac	77.9 ± 2.6
tolmetin	87.8 ± 4.9
vioxx	>100
zomepirac	107 ± 2

[a] K_i values were determined by Dixon plot analyses.

Association of GLO1 with the Anticancer Property of the Indomethacin Family. GLO1-inhibitory activity was observed only in the indomethacin family but not in other classes. GLO1 may play little general role, if any, in antiinflammatory property of the drugs. Instead, GLO1 may be related to some other pharmacological properties unique to the indomethacin family.

One such property may be a beneficial side effect of indomethacin in cancer therapy. A substantial body of clinical and experimental evidence indicates that nonsteroidal antiin-

(21) Thornalley, P. J. *Gen. Pharmacol.* **1996**, *27*, 565−573.
(22) Thornalley, P. J. *Biochem. J.* **1990**, *269*, 1−11.
(23) Gierse, J. K.; Koboldt, C. M.; Walker, M. C.; Seibert, K.; Isakson, P. C. *Biochem. J.* **1999**, *339* (Pt 3), 607−614.

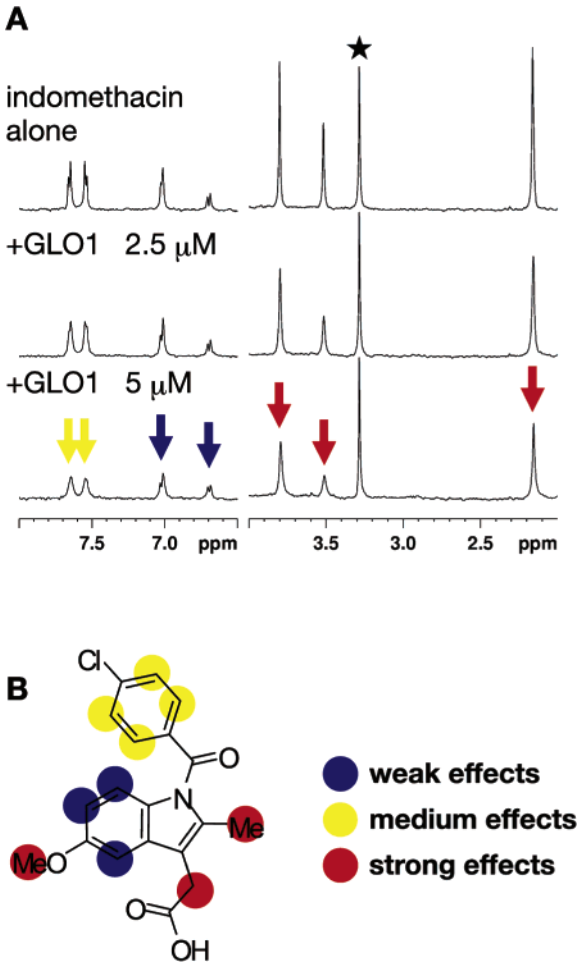

Figure 5. NMR perturbation study. (A) Expanded one-dimensional ^{1}H NMR spectra of indomethacin in the presence or absence of GLO1. Addition of 2.5 μM (middle) or 5 μM (bottom) of GLO1 to a 100-μM NMR sample of indomethacin decreased the signal intensities of the methoxy (3.82 ppm), methylene (3.53 ppm), and methyl (2.18 ppm) protons of indomethacin (indicated by red arrow). A star indicates an internal reference signal arising from methanol. (B) A summary of the differential signal intensities. The percentage value of each signal was calculated by using the internal methanol peak as a reference and classified as strong (red, < the median), medium (yellow, > the median and < the average), and weak (blue, > the average) effects. Detailed data are shown in Supporting Information Figures S4 and S5.

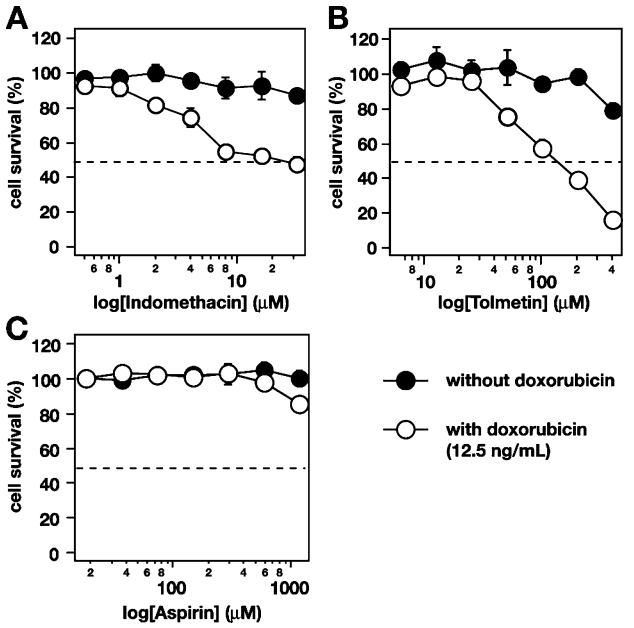

Figure 6. Increased sensitivity of A549 cells to doxorubicin in the presence of indomethacin. A549 cells were treated with three distinct drugs (A, indomethacin; B, tolmetin; C, aspirin) in the presence (open symbols) or absence (filled symbols) of doxorubicin. Cell viability was estimated by WST-1 assays. The data shown are means ± SD for a minimum of three independent experiments.

flammatory drugs including indomethacin have mild anticancer properties as a side effect, especially when combined with chemotherapy.[24−27] Epidemiological studies have also shown that regular use of nonsteroidal antiinflammatory drugs reduces the risk of developing cancers.[27,28] In cultured cells, the indomethacin family, but not other types of nonsteroidal antiinflammatory drugs, potentiates the cytotoxicity of anthracycline anticancer drugs,[29] implying that the property is unique to the indomethacin family. Indomethacin retains such activity against HCT15 human CRC cells (which do not express either COX-1 or COX-2) and *Cox-1/Cox-2*-null transformed murine embryonic fibroblasts.[30] Therefore, the beneficial side effect of indomethacin appears to occur via a COX-independent mechanism.

To evaluate a relationship between GLO1 and the side effect, we chose three antiinflammatory drugs, indomethacin (strong GLO1 inhibition), tolmetin (mild GLO1 inhibition), and aspirin (no GLO1 inhibition) and assayed their ability to enhance the cytotoxicity of doxorubicin, a prototypic anthracycline anticancer drug.[29] Although indomethacin alone had no cytotoxic effects on lung cancer A549 cells up to 32 μM, indomethacin at lower concentrations potentiated the cytotoxicity of doxorubicin (Figure 6A). Tolmetin showed no potentiation of doxorubicin in the same concentration range, but at the higher concentrations (up to 400 μM), tolmetin enhanced the cytotoxicity of doxorubicin (Figure 6B). In contrast, aspirin had no detectable effects even at 1 mM (Figure 6C). These results correspond with the K_i value of the three drugs for GLO1, suggesting that indomethacin sensitizes cells to doxorubicin by inhibiting the enzymatic activity of GLO1.

To further evaluate the role of GLO1 in the synergy of indomethacin and doxorubicin, we modulated expression levels of GLO1 by transfecting its cDNA or siRNA and examined the effects on the drug response. Stable transfection of a GLO1 expression vector into A549 cells yielded three GLO1-overexpressing cell lines that have 1.4- to 6.6-fold expression levels of GLO1 compared with the parental cells (cell line I; 6.6 fold, cell line II; 1.4 fold, and cell line III; 3.8 fold, Figure 7B). When the cells were cotreated with doxorubicin and indomethacin, the cell lines with the higher GLO1 expression were more

(24) Raveendran, R.; Heybroek, W.; Caulfield, M.; Lawson, M.; Abrams, S. M.; Wrigley, P. F.; Slevin, M.; Turner, P. *Hum. Exp. Toxicol.* **1992**, *11*, 291−293.
(25) Maca, R. D. *Anticancer Drug Des.* **1991**, *6*, 453−466.
(26) Ruegg, C.; Zaric, J.; Stupp, R. *Ann. Med.* **2003**, *35*, 476−487.
(27) Hull, M. A.; Gardner, S. H.; Hawcroft, G. *Cancer Treat. Rev.* **2003**, *29*, 309−320.
(28) Hixson, L. J.; Alberts, D. S.; Krutzsch, M.; Einsphar, J.; Brendel, K.; Gross, P. H.; Paranka, N. S.; Baier, M.; Emerson, S.; Pamukcu, R.; et al. *Cancer Epidemiol Biomarkers Prev.* **1994**, *3*, 433−438.
(29) Duffy, C. P.; Elliott, C. J.; O'Connor, R. A.; Heenan, M. M.; Coyle, S.; Cleary, I. M.; Kavanagh, K.; Verhaegen, S.; O'Loughlin, C. M.; NicAmhlaoibh, R.; Clynes, M. *Eur. J. Cancer* **1998**, *34*, 1250−1259.
(30) Zhang, X.; Morham, S. G.; Langenbach, R.; Young, D. A. *J. Exp. Med.* **1999**, *190*, 451−459.

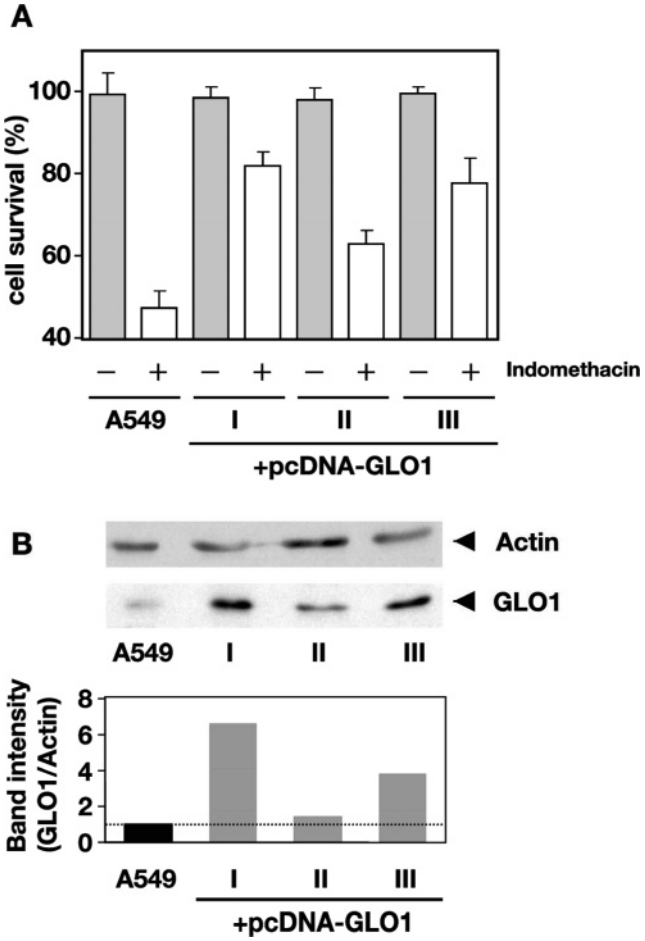

Figure 7. Effects of GLO1 overexpression on the synergy of indomethacin and doxorubicin. Three stable cell lines that overexpress GLO1 at different levels were used (I, II, and III). The expression levels of GLO1 in the cell lines are shown in *B*. (A) A549 cells were treated with a 12.5-ng/mL doxorubicin in the presence (open bars) or absence (gray filled bars) of a 32-μM indomethacin. It is evident that expression of GLO1 decreases the synergy of indomethacin and doxorubicin. The data shown are means ± SD for a minimum of three experiments. (B) Detection of GLO1 by western blot analysis (upper panel). Quantification of GLO1 expression levels (lower panel).

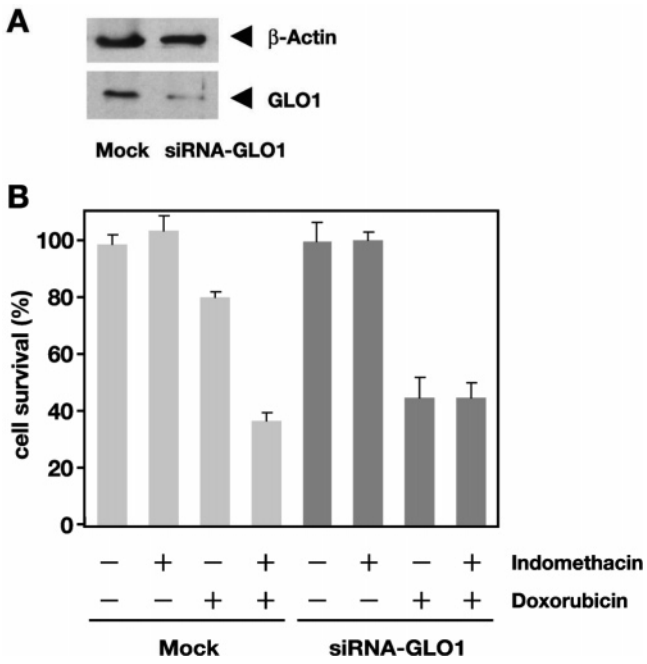

Figure 8. Effects of GLO1 knockdown on the doxorubicin sensitivity. (A) Confirmation of siRNA knockdown of GLO1 in A549 cells. The levels of endogenous GLO1 were analyzed by western blots with an antibody against human GLO1. The β-actin (upper panel) and GLO1 (lower panel) are shown. ~60% knockdown of GLO1 was observed in siRNA-transfected cells. (B) The knockdown of GLO1 replaces indomethacin for increasing sensitivity to doxorubicin. Mock or siRNA-transfected cells were treated with a 16-μM indomethacin in the absence or presence of doxorubicin (6.25 ng/mL). Data were normalized by the viability of cells with no drug treatment.

resistant to the drug treatment than the parental cells (Figure 7A), presumably because the higher concentrations of indomethacin are required for complete inhibition of GLO1 in the overexpressing cells.

Selective silencing of the GLO1 expression was achieved by transiently transfecting GLO1 siRNA (Figure 8A). The GLO1-silenced cells were more sensitive to doxorubicin than the mock-transfected cells were, and indomethacin had limited ability to further potentiate the doxorubicin activity in the GLO1-silenced cells (Figure 8B). Therefore, selective silencing of GLO1 expression replaced indomethacin for enhancing the doxorubicin activity. These results support our notion that inhibition of GLO1 is responsible for indomethacin-mediated enhancement of the doxorubicin activity.

Discussion

Biochemical Isolation of Small Molecule Targets. The small molecules whose target identification provided significant impacts on biology are mostly natural products with potent biological activity, with a few exceptions including those of β blockers[6] and more recently TWS119.[4] The naturally validated bioactive compounds tend to be highly specific toward the gene products with which they coevolved, and therefore natural products have generally been thought more suited for target identification than synthetic molecules have been. However, an increasing number of research tools and drug leads are discovered from phenotypic screening of synthetic compound libraries. Target identification of the synthetic molecules is a bottleneck in chemical genetics and phenotype-based drug discovery.

One drawback of the library-derived compounds is that they are usually not highly potent and may bind several different proteins with low affinity, typically with a K_d of low μM. Successful isolation of these low-affinity targets would increase the value of the library-derived synthetic molecules for biological investigation. In this particular study, the polyproline-linker approach enabled isolation of GLO1 as a target of indomethacin. The K_i and K_d of indomethacin to GLO1 are in a low μM range, but GLO1 inhibition appears to be responsible for the additive effects of indomethacin and anthracyclines on cultured cells and could be relevant to the clinical observation. Our results encourage exploration of low-μM affinity yet pharmacologically relevant targets with affinity-based biochemical purification.

A problem common in natural products and library-derived synthetic compounds is that physiological targets may not be abundant in cell lysates and could be underrepresented on a stained SDS gel. In such a case, high recovery or enrichment of the target is required for the successful isolation.[1] In our particular case, the insertion of a long, rigid polyproline linker

enhanced the recovery of COX-1, a low-abundance protein in cell lysates. Further design of rod-like, and preferably hydrophilic, linkers would increase the success rates of isolating low-abundance proteins.

The generality of the approach needs to be addressed by many other bioactive small molecules including natural products, and such studies are currently underway. We note that the applicability of the polyproline-linker approach may depend on the characteristics of binding proteins. For instance, a biotinylated methotrexate molecule without a proline linker isolated its target, dihydrofolate reductase, at a reasonable yield, and coupling of a proline linker enhanced the isolation only less than 2-fold in our hands (data not shown). The proline-linker approach may prove to be useful for isolating hard-to-isolate proteins.

GLO1 and Indomethacin. Our study identified GLO1 as a binding protein of indomethacin and implicated the inhibition of GLO1 in the sensitization of lung cancer cells to the effects of doxorubicin. Further support for the involvement of GLO1 in the cancer-drug sensitivity can be found in literature. A subtractive gene hybridization study on chemoresistant leukemia cells has shown that GLO1 is overexpressed selectively in the chemoresistant cells, and stable integration of a GLO1 gene into human Jurkat cells rendered the cells resistant to adriamycin, a prototypic anthracycline cancer drug.[31] Increased GLO1 expression has also been found in invasive ovarian,[32] prostate,[33] and breast cancers.[34]

It remains unclear how the inhibition of GLO1 enhances the effects of anthracycline cancer drugs. It is possible to imagine that GLO1 directly reacts and detoxifies the drugs. However, this possibility may be unlikely because 1 day-incubation of GLO1 with doxorubicin had no impacts on the chromatographic and the spectroscopic profile of doxorubicin (data not shown).

A recent study has shown that increased glycolytic flux causes increased methylglyoxal modification of corepressor mSin3A and thereby modulates gene expression.[35] Such methylglyoxal-initiated modulation of gene expression may mediate the synergy between indomethacin and anthracycline cancer drugs.

There is now ample clinical evidence that indomethacin has a number of side effects including the beneficial one in oncology as well as adverse ones such as gastroduodenal ulceration, headache, and dizziness. It is not difficult to suppose that indomethacin interacts with a number of unknown targets that our approach failed to detect. Nonetheless, the finding of GLO1 as an additional target of indomethacin may lead to a better understanding of these pharmacological effects other than antiinflammation and to development of novel anticancer agents or safer derivatives of indomethacin.

Experimental Section

Materials. Mouse embryonic fibroblast STO cells were maintained in DMEM supplemented with 10% FBS. Human lung carcinoma A549 cells were cultured in a 50:50 mixture of Hams F-12:DMEM solution supplemented with 10% fetal bovine serum at 37 °C under humidified 5% CO_2.

Synthesis of 1−7. Conjugates **1**−**7** were synthesized on Rink-Amide MBHA resin (0.6 mmol/g, Nova Biochem) by coupling *N*-α-Fmoc-protected amino acids (Nova Biochem), *N*-ϵ-Fmoc-protected ϵ-aminocaproic acid (Nova Biochem), *N*-Fmoc-amido-dPEG2-acid (Quanta Biodesign), *N*-Fmoc-amido-dPEG4-acid (Quanta Biodesign), *N*-Fmoc-amido-dPEG6-acid (Quanta Biodesign), *N*-Fmoc-amido-dPEG8-acid (Quanta Biodesign), ϵ-maleimidocaproic acid (Pierce), reduced L-glutathione (Sigma-Aldrich), and D-biotin (Sigma-Aldrich) (supplemental Scheme S1), purified by a reversed phase HPLC, and characterized by mass spectrometry and 1d/2d NMR. Conjugate **3**: ^{1}H NMR (D_2O, 600 MHz) δ_H 4.63 (br. t, 9H), 4.59 (br. t, 1H), 4.52 (br. t, 1H), 4.34 (br. m, 2H), 4.15 (t, J=7.2 Hz, 1H), 3.99 (m, 3H), 3.75 (br. m, 9H), 3.54 (br. s, 11H), 3.43 (t, J=6.6 Hz, 5H), 3.25−3.19 (m, 4H), 3.09 (br. m, 6H), 2.63 (br. t, 1H), 2.51 (m, 2H), 2.25−2.12 (m, 12H), 1.95 (t, J=6.6 Hz, 18H), 1.83 (br. t, 11H), 1.51 (br. m, 10H), 1.44 (br. t, 4H), 1.32−1.27 (m, 6H), 1.18 (br. t, 2H); MALDI-TOF−MS Exact mass calcd for $C_{87}H_{131}N_{19}O_{22}S_2^+$ requires *m*/*z* 1858.92. Found *m*/*z* 1858.77. Conjugate **1:** calcd for $C_{42}H_{88}N_{10}O_{13}S_2^+$ requires 985.2. Found (MALDI-TOF−MS) 986.4 $[M + H]^+$. Conjugate **2:** calcd for $C_{72}H_{110}N_{16}O_{19}S_2^+$ requires 1567.9. Found (MALDI-TOF-MS) 1567.6 $[M + H]^+$. Conjugate **4:** calcd for $C_{49}H_{81}N_{11}O_{16}S_2^+$ requires 1144.4. Found (MALDI-TOF-MS) 1144.5 $[M + H]^+$. Conjugate **5:** calcd for $C_{53}H_{89}N_{11}O_{18}S_2^+$ requires 1232.5. Found (MALDI-TOF-MS) 1232.6 $[M + H]^+$. Conjugate **6:** calcd for $C_{57}H_{97}N_{11}O_{20}S_2^+$ requires 1320.6. Found (MALDI-TOF-MS) 1320.6 $[M + H]^+$. Conjugate **7:** calcd for $C_{61}H_{105}N_{11}O_{22}S_2^+$ requires 1408.7. Found (MALDI-TOF-MS) 1408.7 $[M + H]^+$.

Synthesis of 9−13. Conjugates **9**−**13** were synthesized on Rink-Amide MBHA resin (0.6 mmol/g, Nova Biochem) by coupling *N*-α-Fmoc-protected amino acids (Nova Biochem), *N*-ϵ-Fmoc-ϵ-aminocaproic acid (Nova Biochem), indomethacin (Sigma-Aldrich), and D-biotin (Sigma-Aldrich) (supplemental Scheme S2), purified by a reversed phase HPLC and characterized by mass spectrometry. Conjugate **9**: calcd for $C_{79}H_{128}N_{19}O_{15}S^+$ requires 1615.0. Found (MALDI-TOF−MS) 1615.0 $[M + H]^+$. Conjugate **10:** calcd for $C_{53}H_{79}ClN_{11}O_9S^+$ requires 1080.8. Found (MALDI-TOF-MS) 1080.6 $[M + H]^+$. Conjugate **11:** calcd for $C_{98}H_{143}ClN_{20}O_{18}S^+$ requires 1954.8. Found (MALDI-TOF-MS) 1955.1 $[M + H]^+$. Conjugate **12:** calcd for $C_{153}H_{230}ClN_{33}O_{31}S^+$ requires 3095.2. Found (MALDI-TOF-MS) 3095.7 $[M + H]^+$. Conjugate **13:** calcd for $C_{134}H_{217}N_{32}O_{28}S^+$ requires 2755.4. Found (MALDI-TOF-MS) 2755.6 $[M + H]^+$. The concentrations were determined by measuring UV absorbance in methanol (ϵ = 6290 $Lmol^{-1}cm^{-1}$ at λ_{max}=319 nm).

Binding Analysis of Glutathione (GSH)−Biotin Conjugates 1−7. Bacterial lysates were prepared from a 50 mL culture of *E. coli* cells overexpressing glutathione-*S*-transferase (GST) in 2 mL of a lysis buffer [phosphate buffer (pH 7.4) containing 5 mM EDTA, 0.5% NP-40, and 1 mM PMSF]. The soluble fraction was pretreated with Neutravidine-agarose beads to eliminate bacterial biotin-binding and nonspecific proteins. A 150-μL of the pretreated sample was then incubated with each GSH−biotin conjugate (**1**−**7**, 25 μM in a final concentration) at 4 °C for 16 h and added slurry of Neutravidine-agarose beads (100 μL). After another 2-h incubation at 4 °C, the beads were washed three times with the lysis buffer and then three times with a Tris-HCl buffer (pH 8.0) containing 100 mM NaCl. The bound proteins were eluted with a Tris-HCl buffer (pH 8.0) containing 100 mM NaCl and 10 mM reduced L-glutathione, followed by SDS-PAGE.

Isolation of Endogenous COX-1. Mouse STO cells were harvested from a 10-mL culture, resuspended in 500 μL of a binding buffer [phosphate buffer (pH 7.4) containing 100 mM NaCl and 1% DMSO], and sonicated for 5 s three times on ice. Debris was removed by centrifugating the sample at 20000*g* for 30 min. Slurry of Neutravidine-agarose beads (100 μL) saturated with each biotin conjugate was

(31) Sakamoto, H.; Mashima, T.; Kizaki, A.; Dan, S.; Hashimoto, Y.; Naito, M.; Tsuruo, T. *Blood* **2000**, *95*, 3214−3218.
(32) Jones, M. B.; Krutzsch, H.; Shu, H.; Zhao, Y.; Liotta, L. A.; Kohn, E. C.; Petricoin, E. F., 3rd *Proteomics* **2002**, *2*, 76−84.
(33) Samadi, A. A.; Fullerton, S. A.; Tortorelis, D. G.; Johnson, G. B.; Davidson, S. D.; Choudhury, M. S.; Mallouh, C.; Tazaki, H.; Konno, S. *Urology* **2001**, *57*, 183−187.
(34) Rulli, A.; Carli, L.; Romani, R.; Baroni, T.; Giovannini, E.; Rosi, G.; Talesa, V. *Breast Cancer Res. Treat.* **2001**, *66*, 67−72.
(35) Yao, D.; Taguchi, T.; Matsumura, T.; Pestell, R.; Edelstein, D.; Giardino, I.; Suske, G.; Ahmed, N.; Thornalley, P. J.; Sarthy, V. P.; Hammes, H. P.; Brownlee, M. *Cell* **2006**, *124*, 275−286.

incubated with 100 μL of STO cell lysates for 1 h on ice in the binding buffer and washed eight times with the binding buffer. The bound proteins were analyzed by SDS-PAGE, silver staining, and western blots using an antibody against mouse COX-1 (Santa Cruz Biotechnology). For microsequencing of the protein bands, the purification was scaled up 100-fold. A 2-mL solution of the STO-cell lysates prepared from a 1-L culture was incubated with slurry of Neutravidine-agarose beads (1 mL) saturated with biotin conjugates **9** or **11** in the binding buffer on ice for 3 h. After extensive wash with the binding buffer, the bound proteins were eluted with a 1% SDS buffer and separated by SDS-PAGE. The 70-kDa band specific to conjugate **11** was excised from the gel and subjected to LC-MS-MS analysis of tryptic peptides.

Capture and Release of GLO1. A 2-mL solution of the STO-cell lysates prepared from a 1-L culture was incubated with slurry of Neutravidine-agarose beads (1 mL) saturated with biotin conjugates **12** or **13** in the binding buffer [phosphate buffer (pH 7.4) containing 100 mM NaCl (PBS)] on ice for 3 h. After extensive wash with PBS, the beads were treated with 6His-tagged HRV-3C protease (20 units/mL) in PBS at 4 °C for 16 h. The sample was then filtered with an empty polypropylene chromatography column (Biorad). After removal of the protease by using 100 μL of His-Bind resin (Novagen), proteins in the flowthrough were separated by SDS-PAGE. The 25-kDa band specific to conjugate **12** was excised from the gel and microsequenced by LC-MS-MS analysis of tryptic peptides.

Preparation of Recombinant GLO1. Total RNA was extracted from mouse STO cells with ISOGEN-reagent (Nippon Gene), and 5 μg of the RNA was reverse-transcribed to cDNA by using oligo (dT) primer with avian myeloblastosis virus reverse transcriptase (Invitrogen) for 60 min at 42 °C. The reaction mixture was then subjected to PCR by using pfx DNA polymerase (Invitrogen) with following primer pairs: 5′-GGG ATC CCA TAT GGC AGA GCC ACA GCC GGC GTC CAG TGG CCT CAC-3′ and 5′-GAT CGA ATT CCT AAA TAA TCG TTG CTA TTT TGT TAG GAT TCA GAA TCT C-3′. The resulting GLO1 cDNA was then inserted into pET28a expression vector (Novagen) and introduced into *Escherichia coli* BL21-CodonPlus(DE3)-RIPL cells (Invitrogen) for overexpression. Recombinant 6His-taged GLO1 protein was purified by using His-Bind resins (Novagen). Protein concentration was determined using tryptophan and tyrosine absorbance with $\epsilon_{280} = 5500$ and 1100 M^{-1} cm^{-1}.

Determination of K_i Values. The ability of the nonsteroidal antiinflammatory drugs to inhibit the enzymatic activity of mouse recombinant GLO1 was measured in a 50-mM Tris-HCl buffer (pH 6.8) containing 100 mM NaCl, 1% DMSO, 4 mM glutathione, and 4 mM methyl glyoxal (Sigma-Aldrich). After preincubation with varied concentrations of each drug at 30 °C for 10 min, GLO1 (20 nM) was added to the reaction buffer. The rate of formation of *S*-lactylglutathione was monitored by an increase in absorption at 240 nm as described.[36] Data collection was performed below an absorbance of 1.0 to maintain the linearity of the data. Concentrations of the drugs were determined using their λ_{max} absorbance in methanol: acemetacin ($\epsilon_{319} = 6800$ M^{-1} cm^{-1}), aspirin ($\epsilon_{278} = 1300$ M^{-1} cm^{-1}), fenoprofen ($\epsilon_{274} = 1700$ M^{-1} cm^{-1}), ibuprofen ($\epsilon_{265} = 310$ M^{-1} cm^{-1}), indomethacin ($\epsilon_{319} = 6300$ M^{-1} cm^{-1}), ketoprofen ($\epsilon_{255} = 21400$ M^{-1} cm^{-1}), piroxicam ($\epsilon_{255} = 11700$ M^{-1} cm^{-1}), sulindac ($\epsilon_{327} = 15000$ M^{-1} cm^{-1}), tolmetin ($\epsilon_{261} = 9500$ M^{-1} cm^{-1}), and zomepirac ($\epsilon_{256} = 12700$ M^{-1} cm^{-1}).

(36) Lyon, P. A.; Vince, R. *J. Med. Chem.* **1977**, *20*, 77−88.

Overexpression and Knockdown of GLO1. For overexpression of GLO1, pcDNA3.1His(B) expression vector of GLO1 was transfected into A549 cells using Lipofectamine 2000 reagent (Invitrogen). Stable transfectants were selected by G418. For knockdown of GLO1, 21-nucleotide siRNA duplex corresponding to the coding region 99−117 (5′-CAA ACG AUG CUA AGA AUU AdTdT-3′) (Dharmacon Research, Boulder, CO) was transiently transfected using Lipofectamine 2000 reagent (Invitrogen). Expression levels of GLO1 were estimated by Western blot analysis using an antibody against human GLO1 (Abnova) and quantified with the Scion-image (version 4.02) software.

Combination Cytotoxicity Assay. Doxorubicin (LKT Laboratories) was dissolved in DMSO before being diluted to its working concentrations in a culture medium. Acemetacin, aspirin, ibuprofen, indomethacin, ketoprofen, piroxicam, sulindac, and zomepirac sodium (Sigma-Aldrich), and fenoprofen and tolmetin (LKT Laboratories), were dissolved in PBS containing 1% DMSO (pH 7.6) and then were diluted in a culture medium. A549 cells were seeded at 2000 cells per well in 96-well plates, and doxorubicin and each antiinflammatory drug were added on day 2. Four days after the drug addition, cell viability was evaluated by using WST-1 reagent.[29] The results were also confirmed by manual cell counting.

Isothermal Titration Microcalorimetry (ITC) Measurement. The binding of GLO1 to indomethacin was analyzed by a MicroCal VP-ITC calorimeter. A solution of the recombinant mouse GLO1 (10 μM) was titrated with an indomethacin solution (280 μM) or a zomepirac solution (2 mM) at 28 °C in a Tris-buffered saline containing 1% DMSO (TBS: 20 mM Tris, 100 mM NaCl, 1% DMSO, pH 6.8). Binding enthalpy (ΔH), equilibrium-binding constant (K_A), and binding stoichiometry (N) were obtained through the analysis of titration data.

NMR Studies. Indomethacin and methanol was dissolved in PBS containing 5% D_2O at a concentration of 100 μM. Assignments of the proton signals were achieved by 1D and 2D NMR experiments. A PBS solution of GLO1 (100 μM) was gradually added to an NMR sample of indomethacin, and a one-dimensional ^1H spectrum was collected after each addition of the protein. NMR experiments were performed on a Bruker Avance 600 MHz spectrometer. The data were processed using UXNMR (Bruker), and proton chemical shifts were referenced to the H_2O resonance (4.70 ppm at 298 K). The one-dimensional ^1H NMR spectra were recorded with 14 ppm spectral width, 8192 data points, and 298 K temperature. Suppression of the H_2O resonance was achieved by an excitation sculpting gradient pulse.

Acknowledgment. This work was supported in part by grants from NIH (CA109277), Nagase Science and Technology Foundation, and MEXT Scientific Research on Priority Area. We thank A. Otaka for helpful discussion. NMR spectra were obtained in the Keck NMR facility at the University of Houston.

Supporting Information Available: Details of the determination of K_i and K_d values and NMR data (Figures S1−S5), and the synthetic procedures of the polyproline compounds (Schemes S1−S3). This material is available free of charge via the Internet at http://pubs.acs.org.

JA0655643